

Suzuki-Miyaura Coupling Polymerization: Synthesis, Characterization and Optical Properties

Adnan CETIN^{1*}

Highlights:

- The novel thiazole-fluorene based conjugated polymer is synthesized.
- Optic properties of the synthesized polymer were measured such as absorbance, transmittance and optical band gaps.
- This synthesized polymer may be used for applications in optoelectronic devices

Keywords:

- Band edge
- Fluorene
- Optical constant
- Palladium catalyst
- Thiazole

ABSTRACT:

The new thiazole-based polymer was synthesized by the Suzuki-Miyaura crossing-coupling reaction of 5-bromo-N-(3-bromophenyl) thiazol-2-amine and 9,9-dioctyl-9H-fluorene-2,7-diboronic acid bis(pinacol) ester. The synthesized monomer and poly[*N,N'*(1,3-phenylene)bis(thiazol-2-amine)-co9,9'-dioctylfluorene] (Poly[Tm]) were characterized by the Elemental analysis, Fourier Transform Infrared spectroscopy, Nuclear Magnetic Resonance spectroscopy, Thermogravimetric analysis and Gel Permeation chromatography. Furthermore, the optical properties of the Poly[Tm] were studied at three concentrations of 0.625, 1.25 and 2.5 mM in solution. The absorption band edge values of Poly[Tm] decreased with the increasing concentration of the solutions. When the concentration of the Poly[Tm] solution was increased, transmittance values of the Poly[Tm] were increased, and its molar extinction coefficient was resulted in higher absorbance values. Synthesized Poly[Tm] could provide a novel concept for the design of transistors and photovoltaics.

¹ Adnan CETIN (Orcid ID: 0000-0003-4838-1503), Van Yüzüncü Yıl University, Faculty of Education, Department of Chemistry, Van, Turkey

*Corresponding Author: Adnan CETIN, e-mail: adnancetin@yyu.edu.tr

INTRODUCTION

The palladium catalyzed Suzuki-Miyaura (SM) cross coupling reaction is the classical named as one of the most popular selective carbon-carbon bond formation (Das and Linert, 2016, Ye et al., 2017). The cross-coupling reactions to nucleophiles with C-X bond are currently the most widely used for the various C-C bond forming reactions (Halima et al., 2017). The SM reaction was played an important role in organic synthesis and polymer synthesis due to low metal contamination and recyclability (Kotha et al., 2002). Recently, SM coupling reactions were widely used for the design and synthesis of natural products, pharmaceuticals, agrochemicals and advanced functional materials (Isley et al., 2013, Lennox and Lloyd-Jones, 2014, Durak et al., 2016). The SM coupling reactions have assigned a partial structure in many of the industrially important products for preparation of conjugated/functional polymers (Graham et al., 2014). Furthermore, the conjugated polymers were important target molecules in polymer chemistry due to their widespread use in optics such as solar cells, organic photovoltaics, organic light emitting diodes, thin film transistors, and industrial implications (Rivnay et al., 2013, Lakhwani et al., 2014, Samsonidze et al., 2014, Sun et al., 2015). Moreover, the conjugated polymers were known to exhibit various chemical and physical properties such as high electrical conductivity, considerable thermal stability and oxidation resistance as well as the wide range of applications (Bathula et al., 2016, Mehmood et al., 2016, Abdulrazzaq et al., 2017). In addition, the polythiazole structures were an important class of the conjugated polymers (Wilson et al., 2015, Zhang et al., 2016), and the polymers having fluorene moiety has increasingly been received attention in the literature due to their industrial applications (Sui et al., 2014, Hu et al., 2016). Polyfluorene materials were also played a significant role in the material science due to their optoelectronic properties and biophotonics applications (Naga et al., 2014, Xiang et al., 2017).

The value of the band-gap was crucial for light-emitting device (LED) and photovoltaic applications because the band-gap could determine effectiveness in LED devices and photovoltaic devices (Li and Liu, 2014, Muthuraj et al., 2016, Wu and Liu, 2016). Band-gap of the conjugated polymers was a significant adjustable property of the semiconductor materials, and low-band-gap polymers are also available to solar cells as well as n-type conductors and multicolor electrochromic polymers (Tong et al., 2017). Therefore a low-band-gap polymer was primary goal for synthetic chemists. The present study aims (I) to synthesize of the monomer and its polymer, (II) to characterize the monomer and polymer, and (III) to determine of the optical properties at various concentrations of polymer solution.

MATERIALS AND METHODS

Materials

N-(3-bromophenyl)thiazol-2-amine, *N*-bromosuccinimide (NBS), acetonitrile, Magnesium sulfate (MgSO_4), 9,9-dioctyl-9*H*-fluorene-2,7-diboronic acid bis(pinacol) ester, tetrakis(triphenylphosphine)palladium(0), Dimethylformamide (DMF), toluene, diethyl ether, ethyl acetate, hexane, methanol were purchased from Sigma Aldrich (Berlin, Germany) or Merck (Darmstadt, German) companies. All reagents and solvents were used without purification for the determined experiments. The Fourier-transform infrared (FTIR) spectrum was recorded on a Perkin Elmer Precisely Spectrum (Perkin Elmer, Waltham, MA) one spectrometer using pressed disc in the range of $4.000\text{-}450\text{ cm}^{-1}$. ^1H and ^{13}C NMR spectrum were recorded on a Bruker DRX-600 high performance digital FT-NMR spectrometer (Karlsruhe, Germany). Molecular weight and PDI values of the Poly[Tm] were calculated with GPC Agilent 1100 Series (Waldbronn Germany). Optical measurements of Poly[Tm] were determined by a Shimadzu model UV-1800 spectrophotometer in the

wavelength range of 1100-190 nm (Kyoto, Japan). TG measurement values of the Poly[Tm] were carried out by Perkin Elmer Pyris 1 in the range of 20 to 900°C with heating rate of 10°C min⁻¹ under N₂ atmosphere (Seiko, Tokyo, Japan).

Synthesis of 5-bromo-N-(3-bromophenyl)thiazol-2-amine (Tm)

N-(3-bromophenyl)thiazol-2-amine (1.0 eq., 1 mmol, 334 mg) was dissolved to acetonitrile (40 mL) in a Schlenk tube. NBS (1.1 eq., 1.1 mmol, 200 mg) and 3 Å molecular sieve (200 mg) were added to solution at room temperature. The reaction process was stirred at 25°C for 2 h. Then, it was extracted with diethyl ether (3x30 mL). The organic phase was combined water (3x20 mL) and brine (1x20 mL) was added. Organic phase was separated, dried over MgSO₄ and filtered. The combined organic solvents were evaporated under reduced pressure. The crude product was purified by flash column chromatography on silica gel (n-hexane/EtOAc, 10:1). Yield 35%, yellow solid. R_f:0.27 (n-hexane/EtOAc, 10:1). IR spectrum ν , cm⁻¹: 3225 (-NH), 3057 (-C-H_{arom}), 1574 (-C=N). ¹H-NMR spectrum (CDCl₃), δ , ppm: 7.37 (s, 1H, Th-H), 7.03 (d, 1H, Ar-H, *J* = 8.2 Hz), 6.87-6.80 (m, 2H, Ar-H), 6.60-6.51 (m, 1H, Ar-H), 4.31 (s, 1H, -NH), ¹³C-NMR spectrum (CDCl₃), δ , ppm: 154.5, 143.1, 136.3, 130.3, 123.2, 122.7, 119.2, 114.8, 100.4. HRMS spectrum, *m/z*: [M + H]⁺ calcd for C₉H₆Br₂N₂S:333.8317; found:333.8332.

Synthesis of poly[N,N'(1,3phenylene)bis(thiazol-2-amine)-co-9,9'dioctylfluorene] (Poly[Tm])

9,9-dioctyl-9*H*-fluorene-2,7-diboronic acid bis(pinacol) ester (1.0 eq., 1 mmol, 642 mg) and tetrakis(triphenylphosphine)palladium(0) (0.1 eq., 0.1 mmol, 116 mg) were added in three-neck round-bottom flask. The flask was evacuated then filled with argon. After addition of toluene (10 mL) to the flask, a solution of monomer (1.0 eq., 1 mmol, 345 mg) in DMF/H₂O (10/1 mL) and 2 M K₂CO₃ aqueous solution (5 mL) were added. The reaction solution was stirred at room temperature for 48 h. Then, it was extracted with diethyl ether (3x30 mL). The organic phase was combined (3x20 mL). Organic phase was evaporated under reduced pressure. The Poly[Tm] was taken up in toluene/methanol solution. The purification of the Poly[Tm] was done by centrifugation at 6000 g for 15 min and freeze-dried. IR spectrum ν , cm⁻¹: 3210 (NH), 3021 (C-H_{arom}), 2969 (C-H_{aliph}), 1560 (C=C_{arom}), 1493 (C=N), 1313 (C-N), 898 (C-H_{arom}), ¹H NMR spectrum (DMSO-*d*₆), δ , ppm: 7.76 (s, Ar-H), 7.46-7.01 (m, Ar-H), 4.66 (s, N-H), 2.07 (m, -CH₂), 1.75 (m, -CH₃), 1.23 (m, -CH₃). ¹³C NMR spectrum (DMSO-*d*₆), δ , ppm: 161.5 155.6, 148.4, 143.0, 141.5, 139.0, 136.8, 135.3, 133.1, 132.2, 130.6, 129.9, 129.3, 129.2, 128.8, 128.5, 127.2, 121.3, 121.2, 117.8, 109.8, 49.6, 43.7, 35.8, 32.6, 32.2, 29.6, 26.1, 21.5, 19.8, 18.9, 17.4. *M_n* = 3402 g mol, *M_w* = 4103 g mol, (polydispersity index, PDI, 1.21).

RESULTS AND DISCUSSION

Synthesis and Characterization

3-(Tribromomethyl)cyclopentanone starting material (1) was obtained by the reaction with 1,4-adduct of the bromoform and 2-cyclopentenone with lithium bis(trimethylsilyl)amide as strong base at -78 °C according to literature as shown Figure 1 (Choi et al., 2016). To synthesis monomer (Tm), *N*-(3-bromophenyl)thiazol-2-amine (3) in yield 23% was prepared the addition of three equivalent of trimethylamine, 3-(tribromomethyl)cyclopentan-1-one and thiazol-2-amine in tetrahydrofuran as a solvent after at 60 °C 4 h. Then, the bromination of monomer was utilized to NBS, as an electrophilic source of bromine. The reaction to those of acetonitrile bromination with NBS of the *N*-(3-bromophenyl)thiazol-2-amine afforded 5-bromo-*N*-(3-bromophenyl)thiazol-2-amine at room temperature.

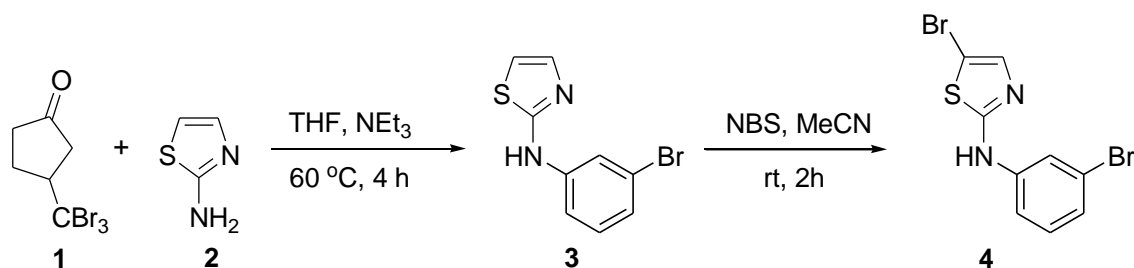


Figure 1. The synthesis of thiazole containing monomer (Tm)

Conjugated polymers are important target organic macromolecules in the polymer synthesis due to the specific chemical and physical properties (Staudt et al., 2022). Moreover, SM coupling reaction is one of the most preferred carbon-carbon bond formations in the palladium-catalyzed cross coupling of the organo boron derivatives with organic electrophiles for polymer chemists due to its reliability, easy accessibility and chemo-selectivity (Chen et al., 2015, Wei et al., 2014). Polymers containing fluorene and thiazole moieties were significant semiconducting materials because of their low band gaps (Miyaura and Suzuki, 1995). For this purpose, a new monomer containing thiazole and dibromide was synthesized as a good leaving group. And a thiazole molecule was indeed an attractive synthon, it was carried out in the preparation dibromide substituents to obtain polymer. Poly[Tm] was synthesized by palladium-catalyzed SM coupling reaction, monomer and 9,9-dioctyl-9H-fluorene-2,7-diboronic acid bis(pinacol) ester in combination with K_2CO_3 as a strong base in Figure 2. The Poly[Tm] reaction was carried out for 48 h. Poly[Tm] was evidenced by GPC. Molecular weight distribution (M_w/M_n) of Poly[Tm] was calculated as 1.21. This provided evidence of a polymerization.

-NH stretching vibration of the amine moieties was observed signal at 3225 cm^{-1} for the monomer. The functional groups C=N asymmetric stretching vibrations and C-H aromatic protons stretching of monomer backbone were corresponding to the bands at 1574 cm^{-1} , 3057 cm^{-1} respectively.

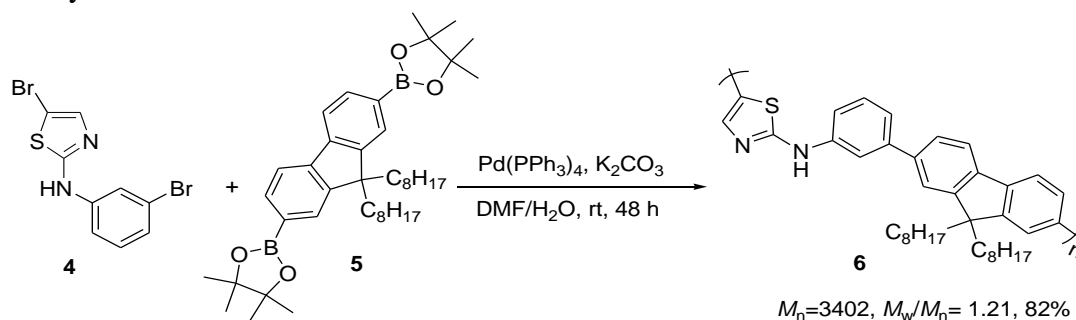


Figure 2. Synthetic route for the synthesis of poly[Tm]

The -CH stretching vibration of the aliphatic groups signal was assigned at 2969 cm^{-1} for the Poly[Tm]. In addition, the amine and aromatic stretching signals in the Poly[Tm] were shifted at 3220 cm^{-1} and 3021 cm^{-1} with regard to monomer. These signals shift could be attributable to the happening of fluorene of the Poly[Tm] (Kaya et al., 2020). The signals of the Poly[Tm] having repeat units and conjugated structures were observed as a broader than monomer in terms of the peak frequencies compared to the monomer IR peaks. The monomer and Poly[Tm] amine protons were observed at δ 4.66 and 4.31 ppm, respectively according to their $^1\text{H-NMR}$ spectra. The NMR peaks of the Poly[Tm] were seen as broad peaks due to the many conjugated structure. The broader peak in the Poly[Tm] was an indication of polymer formation. In addition, the retaining of the peaks of the thiazole, phenyl and fluorene moieties in NMR spectra of the Poly[Tm] showed that the fluorene and thiazole in the Poly[Tm] structures were remained unchanged after polymerization (Jung et al., 2008). The signal

peaks at δ 154.5 and 161.5 ppm related to the $-C=N$ in thiazole ring of the monomer and Poly[Tm] were observed in ^{13}C -NMR spectra. Thermal degradation behaviors of monomer and Poly[Tm] were determined by using a TGA. This process was got through at a range of 25-900 °C by a heating rate of 10 °C / min under nitrogen atmosphere. TGA thermograms and analysis results of the monomer and Poly[Tm] were depicted in Figure 3 and Table 1.

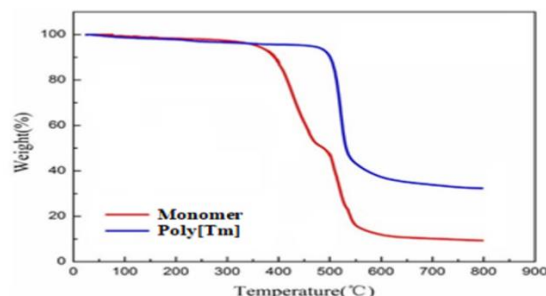


Figure 3. TG curves of Tm and Poly[Tm]

The thermal behavior of the monomer and linear randomly branched Poly[Tm] was investigated using TGA. As to the thermal stability, monomer and Poly[Tm] values showed approximate values in the literature for similar compounds (Santos et al., 2021). Poly[Tm] containing fluorene was thermally stable compared to Tm. The weight losses of monomer and Poly[Tm] were observed as 20% and 53% at 800 °C, respectively. Because of the repeating units, the Poly[Tm] had higher residue than monomer. Synthesized monomer and Poly[Tm] could be occupied as materials in various fields of industry in terms of thermal stable. The long-chain alkyl groups in the Poly[Tm] contributed to the solubility of the prepared material; however, the long-chain alkyl groups showed negative effect in the thermal stability of the Poly[Tm] (Sharma et al., 2015). The conjugated systems could decrease the internal energy of materials. As a result, the Poly[Tm] greatly increased the resistance to high temperature. Furthermore, while σ -bonded polymers were completely degraded at 350-400 °C, Poly[Tm] showed to resist up to 800 °C (Badran et al., 2016).

Table 1. TGA analysis data of the Tm and Poly[Tm]

	^a T _i (°C)	^b T _{50%} (°C)	Weight loss % at 400°C	Weight loss % at 500°C	Weight loss % at 600°C	Weight loss % at 700°C	Weight loss % at 800°C
Tm	300	465	15	49	20	60	3
Poly[Tm]	300	554	7	20	62	64	68

The optical properties of the Poly[Tm]

The polymer studies had attracted much attention thanks for researchers to their optical properties. The optical properties of the Poly[Tm] solutions were determined with a function of wavelength at 0.625, 1.25 and 2.5 mM in the UV-Vis absorbance and transmittance spectra at the 200-1100 nm. The absorbance graph of the Poly[Tm] solution was calculated at various concentrations in solution as shown in Figure 4. It was revealed that the Poly[Tm] solution increased to more absorb in the range of 450-650 nm.

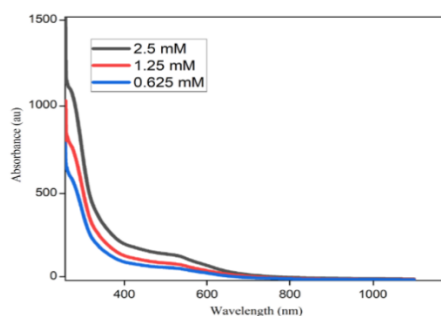


Figure 4. Absorbance spectra of the Poly[Tm] at 0.625, 1.25 and 2.5 mM

Figure 4 showed that the absorbance of the Poly[Tm] solution was observed with absorption by near UV and visible spectrum at various concentrations (0.625, 1.25 and 2.5 mM). When the conjugated polymers were increased conjugation, for optical studies could be suitable tool macromolecules to absorb high wavelengths. The reason for the high wavelength absorption at various concentrations in Poly[Tm] solution was due to its high conjugation structure. The graph against the wavelength of the permeability was depicted in Figure 5a. It was determined that increasing in the transmittance (T) values was noticed with the decreasing concentrations. The addition of water in the Poly[Tm] solution resulted in a decrease of transmittance, and increasing 2-fold added water in the Poly[Tm] solution caused a further decrease of the transmittance. Furthermore, when decreased of transmittance in the UV region (0-650 nm) were detected strong electronic transitions have in the band gap for polymer solutions. The transmittance increased to 630 nm for the Poly[Tm] solutions of various concentrations. The prepared Poly[Tm] solution (0.625 mM) had the highest transmittance of three concentrations. As shown in Table 2, the average transmittance (T_{avg}) values of the Poly[Tm] solutions at 0.625, 1.25 and 2.5 mM were observed as 80.452%, 88.332% and 92.624%, respectively. T_{avg} values of solutions were increased by dilution concentrations of the Poly[Tm] solution. The absorbance band edge (Abs_{be}) of the Poly[Tm] solutions at 0.625, 1.25 and 2.5 mM were calculated using first derivative of the transmittance as shown Table 2 and Figure 5b. Plot λ versus $dT/d\lambda$ for Poly[Tm] solutions was depicted at 0.625, 1.25 and 2.5 mM in Figure 5b. As the molarities the Poly[Tm] solutions increased, it was observed a shifting higher wavelength. The Abs_{be} values were determined to decrease at 0.625, 1.25 and 2.5 mM, and their Abs_{be} values were calculated as 3.654, 3.562 and 3.346, respectively.

Table 2. Direct, Indirect, Forbidden indirect band gap, absorption band edge and T_{avg} values of the Poly[Tm]

No	Concreations (mM)	E_{gd} (eV)	E_{gid} (eV)	E_{gid} (eV)	Absorption band edge (eV)	T_{avg} %
1	0.625	3.937	3.730	3.705	3.654	80.452
2	1.25	3.870	3.646	3.603	3.562	88.332
3	2.5	3.789	3.567	3.462	3.346	92.624

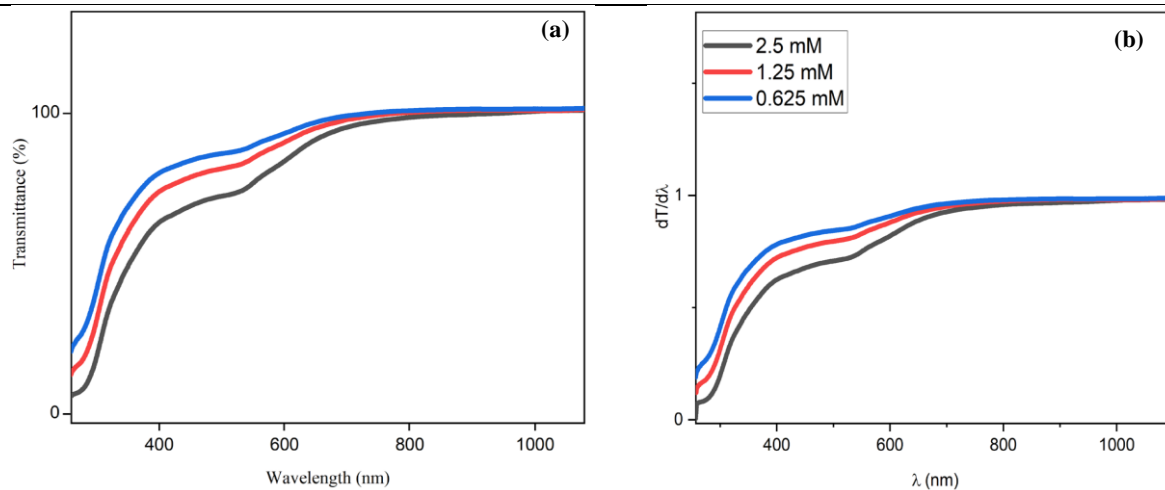


Figure 5. (a) The T versus λ (b) the curves of $dT/d\lambda$ versus λ of the Poly[Tm] solutions at 0.625, 1.25 and 2.5 mM

The optical band gap values of the Poly[Tm] solutions were found by following Tauc equation at 0.625, 1.25 and 2.5 mM by the equation 1 (Cetin et al., 2017;2019).

$$\alpha = A (hv - E_g)^m/hv \quad (1)$$

where α is the absorption coefficient ($h\nu$) is the photon energy. m is a parameter that measure type of band gap, which are values 1/2, 2, 3/2 and 3 (allowed direct, allowed indirect, forbidden direct and forbidden indirect transitions, respectively). A is a constant, as well. The plot $(\alpha \cdot h\nu)^2$ against Energy was depicted to calculate the E_g value of the Poly[Tm] solutions at 0.625, 1.25 and 2.5 Mm as

shown in Figure 6a (see Table 2). It was observed that the semiconductor properties of the Poly[Tm] solutions exhibited the sharp optical absorption features. The Poly[Tm] solution (2.5 mM) was exhibited the lowest the band gap as 3.79 eV. The Poly[Tm] solution (0.625 mM) was the highest band gap value with 3.93 eV in three concentrations. The obtained results mentioned that the band gap values of the Poly[Tm] solutions were decreased in solution of increasing concentration. To observed E_{gid} band gap of Poly[Tm], $(\alpha h\nu)^{1/2}$ against E was plotted in Figure 6b. The E_{gid} band gap values of the Poly[Tm] solutions were calculated as 3.567, 3.646 and 3.730 (eV) at 0.625, 1.25 and 2.5 mM. The situation was similar like E_g values of the Poly[Tm] solutions, in other words, E_{gid} values decreased as the molarity of the Poly[Tm] solution increased. These results were shown that there were direct band gap transitions in the Poly[Tm] solutions at 0.625, 1.25 and 2.5 mM more appropriate than the indirect band gaps transitions.

Figure 7 showed a graph $(\alpha h\nu)^{1/3}$ versus E of the solutions at 0.625, 1.25 and 2.5 mM. The E_{gid} values of the solutions were calculated from zero to value of $(\alpha h\nu)^{1/3}$. E_{gid} values were depicted at 0.625, 1.25 and 2.5 mM in table 2. A graph of wavelength against the molar absorptance coefficient of the Poly[Tm] solutions at 0.625, 1.25 and 2.5 mM was depicted, that was significant to calculate the optical parameters as shown in Figure 8.

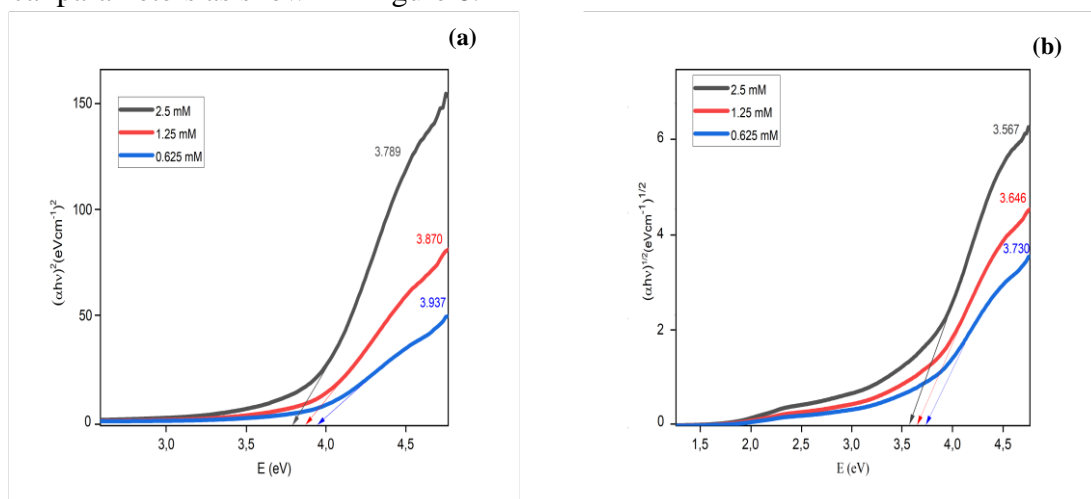


Figure 6. (a) The plots $(\alpha h\nu)^2$ versus E of Poly[Tm] solutions (b) $(\alpha h\nu)^{1/2}$ versus E of Poly[Tm] solutions

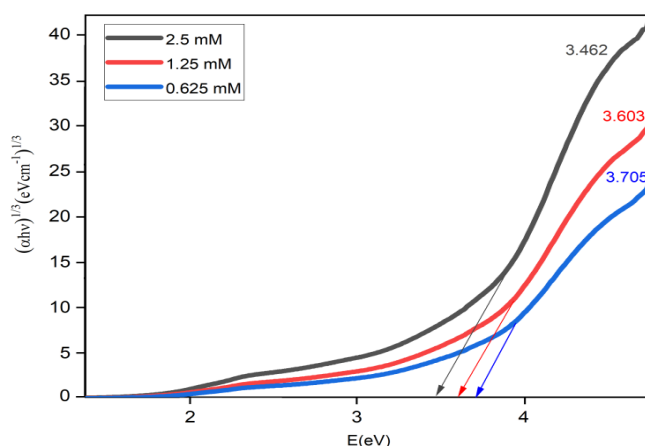


Figure 7. The plot $(\alpha h\nu)^{1/3}$ against E of the Poly[Tm] solutions at 0.625, 1.25 and 2.5 mM

Molar extinction coefficient (ϵ) detected the significant about informations the chemical structure of the synthesized Poly[Tm] (Cetin and Korkmaz, 2018). The molar extinction coefficient values of the solutions were calculated at 0.625, 1.25 and 2.5 mM using a Beer-Lambert scaling relation by the equation 2.

$$\varepsilon = A/cl \quad (2)$$

where c and l are molar concentration and length of the tube, respectively. The molar extinction coefficient values of the solutions have observed the intensity of bands in the near UV and visible region. The ε_{\max} values of the Poly[Tm] solutions at 0.625, 1.25 and 2.5 mM were found to be 1.5×10^3 , 1.9×10^3 and $2.7 \times 10^3 \text{ Lmol}^{-1} \text{ cm}^{-1}$, respectively. The ε_{\max} values of the Poly[Tm] solutions decreased with the increasing concentrations as shown in Figure 8. The mass extinction coefficient (α_{mass}) values of the solutions were determined to following equation for 0.625, 1.25 and 2.5 mM concentrations by the equation 3 (Kuipers and Gruppen, 2007).

$$\alpha = \varepsilon / Ma \quad (3)$$

Molecular mass (Ma) of the Poly[Tm] was 3402 g mol. The ε_{\max} values of the prepared solutions at 0.625, 1.25 and 2.5 mM were calculated as 0.87, 0.62 and 0.48 $\text{Lg}^{-1} \text{ cm}^{-1}$, respectively. It was observed that the maximum α_{mass} values of the Poly[Tm] solutions were decreased with increasing molarity according to obtained results.

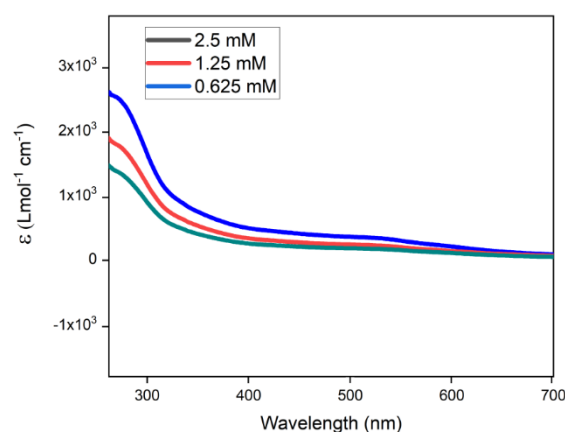


Figure 8. The plot ε_{\max} against λ of the Poly[Tm] solutions at 0.625, 1.25 and 2.5 mM

CONCLUSION

In conclusion, a novel fluorene-thiazole-based conjugated polymer, which could be considered as a potential candidate to develop the photovoltaic materials, was studied in detail in terms of optical properties. The absorbance, transmittance, indirect and forbidden indirect band gap, molar extinction coefficient and mass extinction coefficient values the Poly[Tm] solutions were calculated by the UV-Vis. The optical results revealed that the optical band gap (3.937 eV) of the 0.625 mM Poly[Tm] solution was the highest value in the three solutions. Although, the E_g value (3.789 eV) of the 2.5 mM Poly[Tm] solution was the lowest value in the three solutions. It was observed that low E_g values (direct, indirect and forbidden indirect band gap) were determined raising upon of the Poly[Tm] concentrations. This reduction was caused by the high conjugation and repeat degree as well as the nature of the Poly[Tm]. These values were reduced with the increasing concentration of the Poly[Tm] solutions, consequently, the concentration values were indicated the effect of this reduction on its optical parameters. The Abs_{be} values of the Poly[Tm] solution decreased with the increasing concentration from 3.654 to 3.346 eV. Furthermore, the molar extinction coefficient of the Poly[Tm] was computed, and these values were detected that decreased with increasing concentrations of the Poly[Tm] solutions. The synthesized thiazole-based Poly[Tm] could be good pre-candidate materials for developing new materials in optoelectronic applications.

Conflict of Interest

The author declared that there is no conflict of interest.

REFERENCES

- Abdulrazzaq, M., Ozkut, M. I., Gokce, G., Ertan, S., Tutuncu, E., & Cihaner, A. (2017). A low band gap polymer based on Selenophene and Benzobis (thiadiazole). *Electrochimica Acta*, 249, 189-197.
- Badran, H. A., Hussain, H. F., & Ajeel, K. I. (2016). Nonlinear characterization of conducting polymer and electrical study for application as solar cells and its antibacterial activity. *Optik*, 127(13), 5301-5309.
- Bathula, C., Badgular, S., Belavagi, N. S., Lee, S. K., Kang, Y., & Khazi, I. A. M. (2016). Synthesis, characterization and optoelectronic properties of Benzodithiophene based copolymers for application in solar cells. *Journal of fluorescence*, 26(1), 371-376.
- Ben Halima, T., Zhang, W., Yalaoui, I., Hong, X., Yang, Y. F., Houk, K. N., & Newman, S. G. (2017). Palladium-catalyzed Suzuki–Miyaura coupling of aryl esters. *Journal of the American Chemical Society*, 139(3), 1311-1318.
- Cetin, A. and Korkmaz, A. (2018). Synthesis, optical and morphological properties of novel pyrazole-based oligoamide film. *Optical Materials*, 85, 79-85.
- Cetin, A., Gündüz, B., Menges, N., & Bildirici, I. (2017). Unsymmetrical pyrazole-based new semiconductor oligomer: synthesis and optical properties. *Polymer Bulletin*, 74(7), 2593-2604.
- Cetin, A., Korkmaz, A., Erdoğan, E., & Kösemen, A. (2019). A study on synthesis, optical properties and surface morphological of novel conjugated oligo-pyrazole films. *Materials Chemistry and Physics*, 222, 37-44.
- Chen, L., Wang, K., Mahmoud, S. M., Li, Y., Huang, H., Huang, W., ... & Pietrangelo, A. (2015). Effects of replacing thiophene with 5, 5-dimethylcyclopentadiene in alternating poly (phenylene), poly (3-hexylthiophene), and poly (fluorene) copolymer derivatives. *Polymer Chemistry*, 6(43), 7533-7542.
- Choi, H., Ko, S. J., Kim, T., Morin, P. O., Walker, B., Lee, B. H., ... & Heeger, A. J. (2015). Small-bandgap polymer solar cells with unprecedented short-circuit current density and high fill factor. *Advanced Materials*, 27(21), 3318-3324.
- Das, P., and Linert, W. (2016). Schiff base-derived homogeneous and heterogeneous palladium catalysts for the Suzuki–Miyaura reaction. *Coordination Chemistry Reviews*, 311, 1-23.
- Durak, L. J., Payne, J. T., & Lewis, J. C. (2016). Late-stage diversification of biologically active molecules via chemoenzymatic C–H functionalization. *ACS catalysis*, 6(3), 1451-1454.
- Graham, K. R., Cabanetos, C., Jahnke, J. P., Idso, M. N., El Labban, A., Ngongang Ndjawa, G. O., ... & McGehee, M. D. (2014). Importance of the donor: fullerene intermolecular arrangement for high-efficiency organic photovoltaics. *Journal of the American Chemical Society*, 136(27), 9608-9618.
- Hu, Y., Hu, D., Ming, S., Duan, X., Zhao, F., Hou, J., ... & Jiang, F. (2016). Synthesis of polyether-bridged bithiophenes and their electrochemical polymerization to electrochromic property. *Electrochimica Acta*, 189, 64-73.
- Isley, N. A., Gallou, F., & Lipshutz, B. H. (2013). Transforming Suzuki–Miyaura cross-couplings of MIDA boronates into a green technology: no organic solvents. *Journal of the American Chemical Society*, 135(47), 17707-17710.
- Jung, I. H., Jung, Y. K., Lee, J., Park, J. H., Woo, H. Y., Lee, J. I., ... & Shim, H. K. (2008). Synthesis and electroluminescent properties of fluorene-based copolymers containing electron-withdrawing thiazole derivatives. *Journal of Polymer Science Part A: Polymer Chemistry*, 46(21), 7148-7161.
- Kaya, E., Kurtay, G., & Korkmaz, A. (2020). Combined DFT-experimental investigation and preparation of two new Thiadiazole-based Bithiophene or Fluorene containing polymers via Suzuki-Miyaura reactions. *Journal of Polymer Research*, 27(5), 1-11.
- Kotha, S., Lahiri, K., & Kashinath, D., (2002). Recent Applications of the Suzuki-Miyaura Cross-coupling Reaction in Organic Synthesis. *Tetrahedron*, 58(48), 9633-9695.
- Kuipers, B. J. and Gruppen, H. (2007). Prediction of molar extinction coefficients of proteins and peptides using UV absorption of the constituent amino acids at 214 nm to enable quantitative reverse phase high-performance liquid chromatography–mass spectrometry analysis. *Journal of agricultural and food chemistry*, 55(14), 5445-5451.
- Lakhwani, G., Rao, A., & Friend, R. H. (2014). Bimolecular recombination in organic photovoltaics. *Annual review of physical chemistry*, 65, 557-581.
- Lennox, A. J. and Lloyd-Jones, G. C. (2014). Selection of boron reagents for Suzuki–Miyaura coupling. *Chemical Society Reviews*, 43(1), 412-443.
- Li, K. and Liu, B. (2014). Polymer-encapsulated organic nanoparticles for fluorescence and photoacoustic imaging. *Chemical Society Reviews*, 43(18), 6570-6597.

- Mehmood, U., Al-Ahmed, A., & Hussein, I. A. (2016). Review on recent advances in polythiophene based photovoltaic devices. *Renewable and Sustainable Energy Reviews*, 57, 550-561.
- Miyaura, N., and Suzuki, A. (1995). Palladium-catalyzed cross-coupling reactions of organoboron compounds. *Chemical reviews*, 95(7), 2457-2483.
- Muthuraj, B., Mukherjee, S., Patra, C. R., & Iyer, P. K. (2016). Amplified fluorescence from polyfluorene nanoparticles with dual state emission and aggregation caused red shifted emission for live cell imaging and cancer theranostics. *ACS Applied Materials & Interfaces*, 8(47), 32220-32229.
- Naga, N., Miyanaga, T., & Furukawa, H. (2014). Synthesis and optical properties of organic-inorganic hybrid semi-interpenetrating polymer network gels containing polyfluorenes. *Journal of Polymer Science Part A: Polymer Chemistry*, 52(7), 973-984.
- Rivnay, J., Owens, R. M., & Malliaras, G. G. (2014). The rise of organic bioelectronics. *Chemistry of Materials*, 26(1), 679-685.
- Samsonidze, G., Ribeiro, F. J., Cohen, M. L., & Louie, S. G. (2014). Quasiparticle and optical properties of polythiophene-derived polymers. *Physical Review B*, 90(3), 035123.
- Santos, B. P. S., Lima, A. B., de Araujo, F. L., Mota, I. C., de Castro Ribeiro, A., Nogueira, A. F., ... & Monteiro, S. N. (2021). Synthesis of novel low bandgap random and block terpolymers with improved performance in organic solar cells. *Journal of Materials Research and Technology*, 10, 51-65.
- Sharma, T., Kumar, G. S., Chon, B. H., & Sangwai, J. S. (2015). Thermal stability of oil-in-water Pickering emulsion in the presence of nanoparticle, surfactant, and polymer. *Journal of Industrial and Engineering Chemistry*, 22, 324-334.
- Staudt, M., Cetin, A., & Bunch, L. (2022). Transition Metal-Free Synthesis of meta-Bromo- and meta-Trifluoromethylanilines from Cyclopentanones by a Cascade Reaction. *Chemistry—A European Journal*, 28(10), e202102998.
- Sui, A., Shi, X., Tian, H., Geng, Y., & Wang, F. (2014). Suzuki-Miyaura catalyst-transfer polycondensation with Pd (IPr)(OAc) 2 as the catalyst for the controlled synthesis of polyfluorenes and polythiophenes. *Polymer Chemistry*, 5(24), 7072-7080.
- Sun, M. M., Wang, W., Liang, L. Y., Yan, S. H., Zhou, M. L., & Ling, Q. D. (2015). Substituent effects on direct arylation polycondensation and optical properties of alternating fluorene-thiophene copolymers. *Chinese Journal of Polymer Science*, 33(5), 783-791.
- Tong, J., An, L., Li, J., Zhang, P., Guo, P., Yang, C., ... & Xia, Y. (2017). Large branched alkylthienyl bridged naphtho [1, 2-c: 5, 6-c'] bis [1, 2, 5] thiadiazole-containing low bandgap copolymers: Synthesis and photovoltaic application. *Journal of Macromolecular Science, Part A*, 54(3), 176-185.
- Wei, S., Xia, J., Dell, E. J., Jiang, Y., Song, R., Lee, H., ... & Campos, L. M. (2014). Bandgap engineering through controlled oxidation of polythiophenes. *Angewandte Chemie*, 126(7), 1863-1867.
- Wilson, Z. E., Fenner, S., & Ley, S. V. (2015). Total syntheses of linear polythiazole/oxazole plantazolicin A and its biosynthetic precursor plantazolicin B. *Angewandte Chemie*, 127(4), 1300-1304.
- Wu, T. Y. and Li, J. L. (2016). Electrochemical synthesis, optical, electrochemical and electrochromic characterizations of indene and 1, 2, 5-thiadiazole-based poly (2, 5-dithienylpyrrole) derivatives. *RSC advances*, 6(19), 15988-15998.
- Xiang, C., Wan, H., Zhu, M., Chen, Y., Peng, J., & Zhou, G. (2017). Dipicolylamine functionalized Polyfluorene based gel with lower critical solution temperature: preparation, characterization, and application. *ACS Applied Materials & Interfaces*, 9(10), 8872-8879.
- Ye, Y. X., Liu, W. L., & Ye, B. H. (2017). A highly efficient and recyclable Pd (II) metallogel catalyst: A new scaffold for Suzuki-Miyaura coupling. *Catalysis Communications*, 89, 100-105.
- Zhang, Q., Li, Y., Lu, Y., Zhang, H., Li, M., Yang, Y., ... & Li, C. (2015). Pd-catalysed oxidative C-H/C-H coupling polymerization for polythiazole-based derivatives. *Polymer*, 68, 227-233.